Effect of Die Geometry on Foaming Behaviors of High-Melt-Strength Polypropylene with CO_2

Patrick C. Lee,[1] Wanrudee Kaewmesri,[2] Jing Wang,[1] Chul B. Park,[1] Jantrawan Pumchusak,[3] Rick Folland,[4] Andreas Praller[5]

[1]*Microcellular Plastics Manufacturing Laboratory, Department of Mechanical and Industrial Engineering, University of Toronto, Toronto, Ontario, Canada M5S 3G8*
[2]*Department of Materials Science, Faculty of Science, Chiang Mai University, Muang, Chiang Mai 50200, Thailand*
[3]*Department of Industrial Chemistry Science, Faculty of Science, Chiang Mai University, Muang, Chiang Mai 50200, Thailand*
[4]*Borealis Polymers N.V., Industrieweg 148, B-3583 Beringen, Belgium*
[5]*Linde AG, Linde Gas Division, Development and Application Technology Plastic Industry, 85716 Unterschleissheim, Germany*

Received 1 August 2007; accepted 11 December 2007
DOI 10.1002/app.28204
Published online 23 May 2008 in Wiley InterScience (www.interscience.wiley.com).

ABSTRACT: This article reports on a systematic study that was conducted to investigate the effects of die geometry (i.e., pressure and pressure drop rate) on the cell nucleation and growth behaviors of noncrosslinked high-melt-strength (HMS) polypropylene (PP) foams blown with supercritical CO_2. The experimental results showed that the cellular morphologies of PP foams were sensitive to the die geometry. Furthermore, the initial expansion behavior of the foam extrudate at the die exit was recorded using a high-speed CCD camera. This enabled us to achieve a more thorough understanding of the effect of die geometry on both the initial expansion behavior and the final cellular morphology of HMS PP foams. The effect of die temperature on cell morphology was also studied. © 2008 Wiley Periodicals, Inc. J Appl Polym Sci 109: 3122–3132, 2008

Key words: branched; foam extrusion; poly(propylene) PP

INTRODUCTION

Thermoplastic foams exhibit a two-phase cellular structure (i.e., a solid polymer matrix and a gaseous phase) created by the expansion of a blowing agent. This cellular structure provides unique properties, such as light weight and low thermal conductivity, which enable foamed plastics to be used effectively for various industrial applications.[1] Because of the outstanding functional characteristics and relatively low material costs, PP foams have been considered to be one of the most promising candidates among thermoplastic foams for industrial applications. PP is resistant to chemicals and abrasion, and has a number of advantages over polystyrene and polyethylene[2]: PP materials have a higher rigidity compared with other polyolefins; they offer better strength than polyethylene and better impact strength than polystyrene; and they provide higher service temperature and good temperature stability. Only limited research has been conducted, however, on the production of PP foams; their weak melt strength means that they are more difficult to manufacture compared with the other plastics.[3]

Most polyolefin foams are produced by the free expansion process, which is based on the theory that the gaseous phase, which is dispersed throughout the polymer melt, expands at the die exit. The gaseous phase may be generated by the separation of a dissolved gas, the vaporization of a volatile liquid, or the release of gas from a chemical reaction. Regardless of the type of blowing agent, the expansion process comprises three major steps: (i) nucleation; (ii) bubble growth; and (iii) stabilization. The nucleation phase (i.e., the formation of expandable bubbles) begins in a polymer melt that has been supersaturated with a blowing agent. Once a bubble reaches a critical size, it continues to grow as the blowing agent rapidly diffuses into it. This growth continues until the bubble stabilizes or ruptures.[4]

When cell nucleation takes place in the extrusion foaming die, the cells grow and the foam density decreases (i.e., the void fraction increases) as the available blowing agent molecules diffuse into the cells. In general, cell growth is affected primarily by: the time allocated for them to grow; the temperature of the system; the state of supersaturation; the hydrostatic pressure or stress applied to the polymer

Correspondence to: C. B. Park (park@mie.utoronto.ca).

matrix; and the viscoelastic properties of the polymer/gas solution.[5–7]

Since foam products made from linear PPs usually have limited expansion capabilities due to their weak melt strength, material modifications and new resin developments have been actively researched to improve their foamability. Earlier efforts have included crosslinking PP resins, which significantly improved volume expandability, cell uniformity, and thermoformability.[8–11] Other researches has entailed promoting long-chain branching[12–16] to improve the melt strength of PP materials. Significantly improved foamability and thermoformability were observed from long-chain branched high-melt-strength (HMS) PP resins.[3,12,13,17,18] Various other grades of HMS PP polymers have also been produced and studied.[19–21]

Recently, the automotive industry has demonstrated significantly increased interest in the manufacture of recyclable noncrosslinked PP foams to replace the existing crosslinked PP foams currently used in many applications. Furthermore, using environmentally benign and inexpensive CO_2 as a blowing agent in PP foaming has become preferable to using long-chain blowing agents such as HCFCs, HFCs, pentane, and butane. Up until now, these long-chain, physical blowing agents have been employed in low-density foam processing because of their low diffusivity and high solubility.[4] This low diffusivity offers a tremendous advantage as it allows for controlled cell growth in which a very high expansion ratio (up to 90-fold) can be achieved;[22,23] it is easy to regulate cell growth in these cases because the growth rate is slow and gas escape can be prevented easily. CFCs and HCFCs, however, are known to be environmentally hazardous, and their use has been prohibited from foaming industries. The use of pentane and butane has also been limited due to their high flammability. As a result, gaseous blowing agents, such as CO_2 and N_2, have recently been heralded as alternatives to long-chain blowing agents in plastic foam processing. These gaseous blowing agents were used to manufacture relatively high-density foams with volume expansion ratios in the range of 1.2- to 15-fold (although mainly less than 10-fold).[24–32] Many patents describe well-known methods of inert gas-based foam processing for the manufacture of relatively high-density foams.[26–32] Since the inert gas blowing agents have higher volatility (and thereby higher diffusivity) than the long-chain blowing agents, gaseous blowing agents can escape easily during expansion.[33,34] Therefore, it is very challenging to obtain low-density foams with an expansion ratio of over 15-fold using an inert gas as the blowing agent. They have been effectively used, however, to produce fine-celled or microcellular foams because of their high volatilities.[5,35–37]

The foaming behaviors of various PP resins have been investigated. The cell nucleating behavior and the final cell density of extruded PP foams with various nucleating and blowing agents have also been studied extensively for fine-celled PP foam applications,[3,38–43] as have the volume expansion behavior and the final foam density in the context of low-density PP foam applications.[44–50] The fundamental expansion mechanisms of gas loss and melt stiffening for PP foam processing have been identified.[7,51] Despite all the research that has been conducted on the cell nucleation and cell growth of PP materials, to the best of our knowledge there has been no systematic investigation carried out on the effect of die geometry (i.e., pressure and pressure-drop rate) on the cell nucleation and cell growth behaviors of PP foams with CO_2.

This article reports on an experimental study that was conducted to investigate the fundamental cell growth mechanisms of extruded HMS PP foams with CO_2 as a blowing agent. In particular, this research focuses on the effects of the die geometry on the volume-expansion behaviors of PP foams. The die geometry and CO_2 contents were varied and the foam extrudate at the die exit was visualized at the early stage using a CCD camera to observe the initial expansion behavior of the extrudate.

BACKGROUND ON THE GOVERNING MECHANISMS OF VOLUME EXPANSION OF PP FOAMS

Naguib et al.[7,51] have claimed that the final volume expansion ratio of the extruded PP foams blown with *n*-butane was governed by two main mechanisms: (i) the loss of the blowing agent through the foam skin at high temperatures, and (ii) the crystallization of the polymer matrix at low temperatures.

The gas loss phenomenon is a dominant factor that constrains the maximum volume expansion when the melt temperature is high. The diffusivity of blowing agents at elevated temperatures is generally very high. Therefore, if the processing temperature is too high, the gas can easily escape from the extruded foam because of its higher diffusivity at elevated temperatures. Furthermore, as the foam expands, the cell wall thickness decreases and the resulting rate of gas diffusion between cells increases even more. Consequently, the rate of gas escape from the foam to the environment increases significantly. Gas escape through the thin cell walls decreases the amount of gas available for cell growth, which results in lower final expansion. Moreover, if the cells do not freeze quickly enough, they tend to shrink due to severe gas loss through the foam skin, which causes overall foam contraction.

The crystallization of PP foams at low temperatures is another critical factor that affects the maximum expansion ratio. For semicrystalline polymers such as PP, the polymer melt solidifies at the moment of crystallization during cooling. Ultimately, then, the PP foam structure ''freezes'' at the crystallization temperature during the foaming process. If the crystallization occurs in the primitive foaming stage (i.e., before the dissolved blowing agent has fully diffused out of the plastic matrix and into the nucleated cells), then the foam cannot be fully expanded. Furthermore, the cell walls become too stiff for the gas to expand. Therefore, to achieve the maximum volume expansion ratio from the PP foam, crystallization should be prevented from occurring before all the dissolved gas diffuses out into the nucleated cells and the foam expands to its maximum capacity. Upon exiting the die, the temperature of the melt decreases as a result of the external cooling that takes place outside the die and the cooling effect that transpires due to the isentropic expansion of the blowing gases. Thus, the processing temperature at the die determines the time after which the polymer melt solidifies. As such, to allow enough time for the gas to diffuse into the polymer matrix, the processing temperature should be maintained at an appropriately temperature.

This suggests that there is an optimum processing temperature for achieving maximum expansion. If the melt temperature (i.e., the processing temperature) is too high, then the maximum volume expansion ratio is governed by gas loss, and the volume expansion ratio will increase as the processing temperature decreases. If the processing temperature is too low, then the volume expansion ratio is governed by the crystallization of PP; the volume expansion ratio will thus increase as the temperature increases. Consequently, it is expected that the volume expansion mechanisms that characterize PP foams with blown with *n*-butane should be applicable to the foam processing HMS PP blown with CO_2.

DIE DESIGN AND CALIBRATION

The purpose of effective die design is to be able to actively control the geometries of the filamentary dies (i.e., the die diameter and the die length) so that they will present the effects of different die pressures and different pressure drop rates on the final foam structures. Modeled on Xu et al.,[52] who designed three interchangeable groups of nine dies with the same pressure or the same pressure drop rate, we designed similar sets of dies in this study. Xu et al. assumed that a ''power law'' model could describe the polymer melt, and that the theoretical die pressures and pressure drop rates could be calculated using eq. (1) through (3):[53]

$$P_{\text{die}} = -2m\frac{L}{R^{3n+1}}\left[\left(3+\frac{1}{n}\right)\frac{Q}{\pi}\right]^n \tag{1}$$

$$t_{\text{residence}} \approx \frac{L}{v_{\text{avg}}} = \frac{L}{Q/\pi R^2} = \frac{\pi R^2 L}{Q} \tag{2}$$

$$\frac{dp}{dt} \approx \frac{P_{\text{die}}}{t_{\text{residence}}} = -2m\left(3+\frac{1}{n}\right)^n\left(\frac{Q}{\pi R^2}\right)^{n+1} \tag{3}$$

Equation (1) expresses the pressure drop along the capillary die land with a constant cross section; eq. (2) expresses the average residence time inside the capillary; and eq. (3), obtained by dividing eq. (1) over eq. (2), expresses the pressure drop rate.

Since the material used in this study is different from that of Xu et al.,[52] the geometrical parameters of the dies have to be recalculated. We specified three different die pressure levels: 6.9 MPa (1000 psi), 13.8 MPa (2000 psi), 20.7 MPa (3000 psi). At the same time, three different pressure drop rates were chosen at 155 MPa/s, 48 MPa/s, and 7.2 MPa/s. Compared with the Xu et al.,[52] the chosen pressures and pressure drop rates were lower such that the possibility of achieving a high expansion ratio at a lower cell density could be studied.

The power law parameters that describe the shear-thinning behavior of PP without CO_2 were determined to be $m = 2100\ N\ s^{0.51}/m^2$ and $n = 0.51$. These parameters were measured on a capillary rheometer at 190°C. Data was then fitted in a least square method over a shear rate range of 20 s^{-1} to 2000 s^{-1}. A flow rate of 13 g/min was chosen; the latter is a typical flow rate value for extrusion studies. The calculated geometries of the eight filamentary dies are summarized in Table I and illustrated in Figure 1.

The initially designed dies had to be calibrated for our experiments for two main reasons. First, the polymer would undergo a very different processing trajectory in our tandem system compared to that in a capillary rheometer. Because of the long residence time and path length inside the extruder and the gear pump, the extruded polymer may have a different viscosity from that of the virgin polymer.[54] Second, the entrance pressure drop from the upstream reservoir into the capillary die land was not considered in this set of experiments.[55] The calibration process involves running pure polymer through dies of the same group (e.g., Die 1, 2, and 3) at exactly the same processing condition and compare die pressure. After removing excessive capillary length using a lathe, dies of the same group should have linearly increased capillary lengths and linearly increased die

TABLE I
Calculated Geometry, Residence Time, and Pressure Drop Rate of the Dies for HMS PP

Die group	Die no.	Pressure drop level, MPa (psi)	Die diameter, mm (inch)	Die length, mm (inch)	Average residence time (ms)	Pressure drop rate (MPa/s)
Group 1	Die 1	6.9 (1000)	0.940 (0.037)	12.79 (0.50)	4.44E + 1	1.55E + 2
	Die 2	13.8 (2000)	0.940 (0.037)	25.70 (1.01)	8.92E + 1	1.55E + 2
	Die 3	20.7 (3000)	0.940 (0.037)	38.61 (1.52)	1.34E + 2	1.55E + 2
Group 2	Die 4	6.9 (1000)	1.219 (0.048)	24.73 (0.97)	1.44E + 2	4.80E + 1
	Die 5	13.8 (2000)	1.219 (0.048)	49.70 (1.96)	2.90E + 2	4.80E + 1
	Die 6	20.7 (3000)	1.219 (0.048)	74.68 (2.94)	4.35E + 2	4.80E + 1
Group 3	Die 7	6.9 (1000)	1.854 (0.073)	71.30 (2.81)	9.62E + 2	7.2
	Die 8	13.8 (2000)	1.854 (0.073)	143.3 (5.64)	1.93E + 3	7.2

pressures. In fact, following capillary rheometry, the pressure difference between dies of the same group were converted to melt viscosity using standard formulas,[53] and these viscosities were similar to those measured on capillary rheometer at the same temperature. The calibrated die geometries are shown in Table II.

ANALYSIS OF PREMATURE CELL GROWTH AND ITS INFLUENCE ON FOAM STRUCTURES

The expansion ratio that can be achieved during extrusion is determined chiefly by the flow rate, the die temperature, the die pressure, and the pressure drop rate. One approach to studying these parameters is to calculate the amount of premature cell growth that occurs during foaming. As the polymer melt is squeezed through the die land, its pressure drops linearly due to the constant die cross section. At a certain moment, the melt pressure falls below the solubility pressure, which is the minimum pressure level required to prevent any phase separation; at this point, cell nucleation and growth begin to take place. The amount of gas that has diffused out of the polymer melt before it emerges from the die exit is very detrimental to the final expansion ratio because the diffused gas will rapidly escape from the extrudates' surface before it has solidified.[7,56] Moreover, premature cell growth gives rise to unwanted cell coalescence and mars the surface of the final extrudate as a result of high gas diffusivity and weak polymer strength at high temperatures.

Xu and Park used a series of filamentary dies to analyze the amount of premature cell growth that may occur during PS extrusion.[57] Using a similar approach, we assumed that the amount of gas that diffuses into a cell is limited to a hypothetical sphere called the ''depleted region,'' whose radius was determined by the gas diffusion distance during premature cell growth. The diffusion distance is defined as:

$$l \approx \sqrt{D(T) \times t_{\text{premature}}} \tag{4}$$

where $D(T)$ is the temperature-dependent mutual diffusivity coefficient of the PP/CO_2 system, and $t_{\text{premature}}$ is the premature cell growth time i.e., the time between cell nucleation and the emergence of the extrudate from the die exit.[36] The premature cell growth time can be calculated if we assume that the PP/CO_2 mixture pressure drops linearly along the die land (i.e., by ignoring the viscosity change during phase separation):

$$t_{\text{premature}} = \frac{P_{\text{solubility}}(C_s, T)}{P_{\text{die}}} \times t_{\text{residence}} = \frac{P_{\text{solubility}}(C_s, T)}{dp/dt} \tag{5}$$

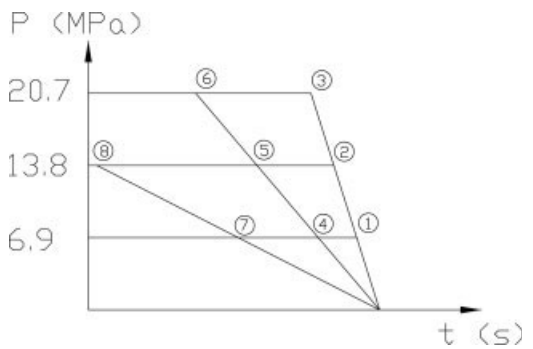

Figure 1 Targeted pressure drop and pressure drop rate for the 8 filamentary dies for HMS PP.

TABLE II
Calibrated Geometry of the Dies for HMS PP

Die group	Die no.	Die diameter, mm (inch)	Die length, mm (inch)
Group 1	Die 1	0.940 (0.037)	7.50 (0.295)
	Die 2	0.940 (0.037)	17.03 (0.670)
	Die 3	0.940 (0.037)	26.1 (1.028)
Group 2	Die 4	1.219 (0.048)	14.64 (0.576)
	Die 5	1.219 (0.048)	29.36 (1.156)
	Die 6	1.219 (0.048)	44.55 (1.754)
Group 3	Die 7	1.854 (0.073)	48.21 (1.898)
	Die 8	1.854 (0.073)	121.07 (4.767)

where the solubility pressure, $P_{\text{solubility}}(C_s, T)$, is a function of gas concentration and temperature. Other parameters have been explained in the previous section.

Finally, the amount of premature cell growth is calculated as:

$$M_{\text{premature}} = Nm_p + M_{p_0} = N \times C_s \times \frac{4}{3}\pi l^3 + M_{p_0} = N \times C_s \times \frac{4}{3}\pi\left(\frac{D(T)\times P_{\text{solubility}}(C_s, T)}{dp/dt}\right)^{3/2} + M_{p_0} \quad (6)$$

where N is the average cell density during premature cell growth; m_p is the amount of gas diffused into a single cell; and M_{p0} is the amount of undissolved gas (due to low die pressure or poor mixing in the extrusion system). Since eq. (6) ignores the gas concentration gradient at the cell/polymer interface, it tends to slightly overpredict the amount of premature cell growth.

In eq. (6), N is readily obtained from the cell density measured from the extrudates (see Fig. 5). To calculate diffusivity, the normalized sorption curves from solubility experiments were employed.[58] The values for $D(T)$ of the PP/CO_2 system were calculated at 453, 473, and 493 K were extrapolated to the optimal processing temperatures (usually 423 K) using an exponential function (i.e., $D(T) = D(T_0) \times \exp(-A/T)$, where T_0 is a reference temperature, and A is a fitting parameter).[59] The diffusivity at 423 K was determined to be 6×10^{-9} m^2/s.

The solubility pressures were estimated based on the work of Li et al.[58] Their reported equilibrium pressures at low CO_2 concentrations can be fitted to a linear function:

$$P_{\text{solubility}} = -469.117 + 2.7541 \times T + 172.539 \times C \quad (7)$$

where T is the temperature and C is the equilibrium CO_2 concentration in PP.

To calculate dp/dt, we used the residence time calculated from eq. (2) and the actual die pressure readings during experiments. Figure 2 shows the calculated amount of premature cell growth (as a percentage of the total gas content) as a function of the pressure drop rate. In general, the amount of premature cell growth decreases as the pressure drop rate increases. This is attributed to the shorter residence time in higher dp/dt dies with smaller cross sections. The amount of premature cell growth is also influenced by the total gas content, since higher gas content implies a higher solubility pressure.

It was observed that the solubility pressure for 5 wt % of CO_2 at the optimal processing temperature, measured in a static magnetic suspension balance, was ~ 800 psi. However, we suspect that the actual pressure threshold to keep all CO_2 dissolved should be higher than 800 psi due to two reasons: First, the estimated volume swelling due to CO_2 dissolution, used in the calculation of solubility pressure, is not supported by experimental results; Second, solubility pressure in shear flow is different from that in a static condition (i.e., shear induced nucleation[6]). Research on this topic is very immature now and will not be elaborated here. As such, we surmised that the low-pressure dies (dies 1, 4, and 7) would incorporate a certain amount of undissolved CO_2. We believed that undissolved CO_2 existed in the form of tiny bubbles, and replaced heterogeneous nucleation sites (i.e., talc) when die pressures decreased. As a result, oversaturated CO_2 will diffuse into existing gas bubbles instead of forming new bubbles through heterogeneous nucleation. This low cell density promotes cell coalescence and collapse, and contributed significantly to the collapse of the expansion ratios. For experiments with 1 and 3 wt % of CO_2, it was estimated that all the gas was dissolved, and that premature cell growth played a negligible role in determining the cell morphology.

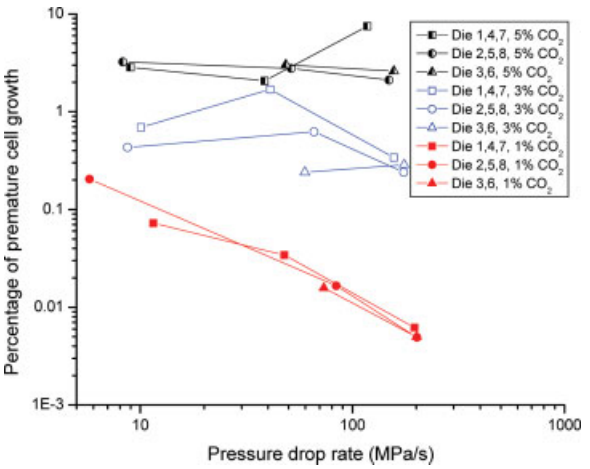

Figure 2 Premature cell growth amount obtained at the optimal processing temperature as a function of the pressure drop rate. [Color figure can be viewed in the online issue, which is available at www.interscience.wiley.com.]

The above calculations, although informative, involved several approximations. First, the cell density of the extrudates did not reflect the average cell density inside the die. It was believed that this cell density was much lower than the initial cell nucleation density, and that the cells would coalesce and collapse before they stabilized and achieved a final cell structure. Second, the entrance pressure drops were ignored in our calculations. In reality, this usually equals the pressure drop over a die land length of 5–10 times the capillary diameter.[55] These two factors reflect an underestimation of the amount of

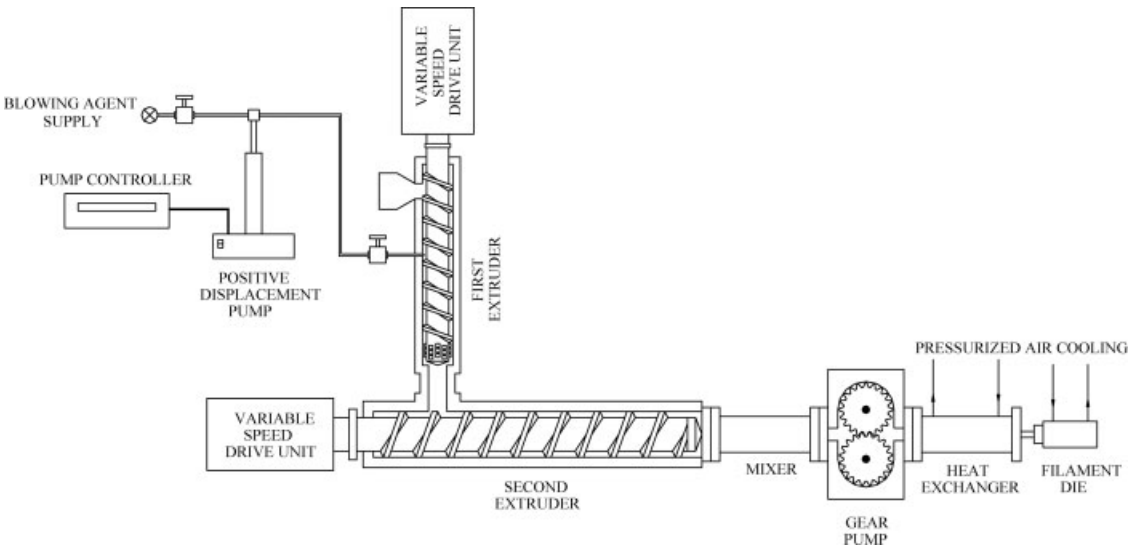

Figure 3 Schematic of the experimental system setup.

premature cell growth, and are believed to dominate over other factors in determining the accuracy of the above model.

EXPERIMENTAL

Experimental materials

The plastic material used in this study was HMS PP (WB135HMS, MFI = 2.3 g/10 min) and was supplied by Borealis Gmbh. The foaming additive was talc, which also doubled as a cell nucleating agent. Talc with a top-cut of 7 μm was used in a master batch of 20 wt % concentration and was provided by Borealis Gmbh. The CO_2, supplied by BOC Gas (The Linde Group), was utilized as a blowing agent. The CO_2 was a commercial grade with minimum 99.5% purity, where the sum of trace N_2, O_2, and CH_4 was less than 0.5%.

Experimental setup

Figure 3 shows a schematic of the tandem extrusion system used in this study. It consists of the following components: a 5 hp extruder driver with a speed control gearbox (Brabender: prep center); one 3/4'' extruder (Brabender: 05-25-000) with a mixing screw; one 1½'' extruder with a built-in 15 hp variable speed drive unit (Killion: KN-150); a positive displacement pump for injecting the blowing agent into the polymer melt; a gear pump (Zenith PEP-II 1.2 cm^3/rev); a heat exchanger for cooling the polymer melt, which contains homogenizing static mixers; a filament die with various length/diameter (L/D) ratios (summarized in Table II); and a cooling sleeve to achieve precise control of the die temperature. The first extruder is used for plasticating the polymer resin. The second extruder mixes the polymer melt and subsequently subjects it to an initial cooling period. The gear pump controls the polymer melt flow rate, independent of temperature and pressure changes. The heat exchanger provides further cooling for the polymer melt to suppress cell coalescence. Finally, shaping and foaming occur in the filament die. In our experiment, an on-line progressive scan imaging system was mounted at the die exit. Using a frame grabber and image processing software, we succeeded in capturing images of the extrudate as it came out of the die. The progressive scan imaging system consists of a CCD camera (CV-M10), which has a very high shutter speed (up to 1/800,000 s), with a magnifying lens (Navitar), a frame grabber (PC vision), and image processing software (Sherlock).

Experimental procedure

The PP pellets, mixed with a fixed amount of talc (i.e., 0.8 wt %), were first fed into the barrel through the hopper and were completely melted by the motion of the screw. A designated amount of CO_2 (i.e., 1, 3, or 5 wt %) was then injected into the extrusion barrel by a positive displacement pump, mixed with the polymer melt stream in the barrel, and eventually dissolved in the melt. When the gas was injected into the extrusion barrel, the remaining section of the first screw and the second screw generated shear fields that completely dissolved the gas in the polymer melt via convective diffusion. The single-phase polymer/gas solution went through the gear pump and was fed into the heat exchanger where it was cooled to the desired temperature. The cooled polymer/gas solution entered the die and

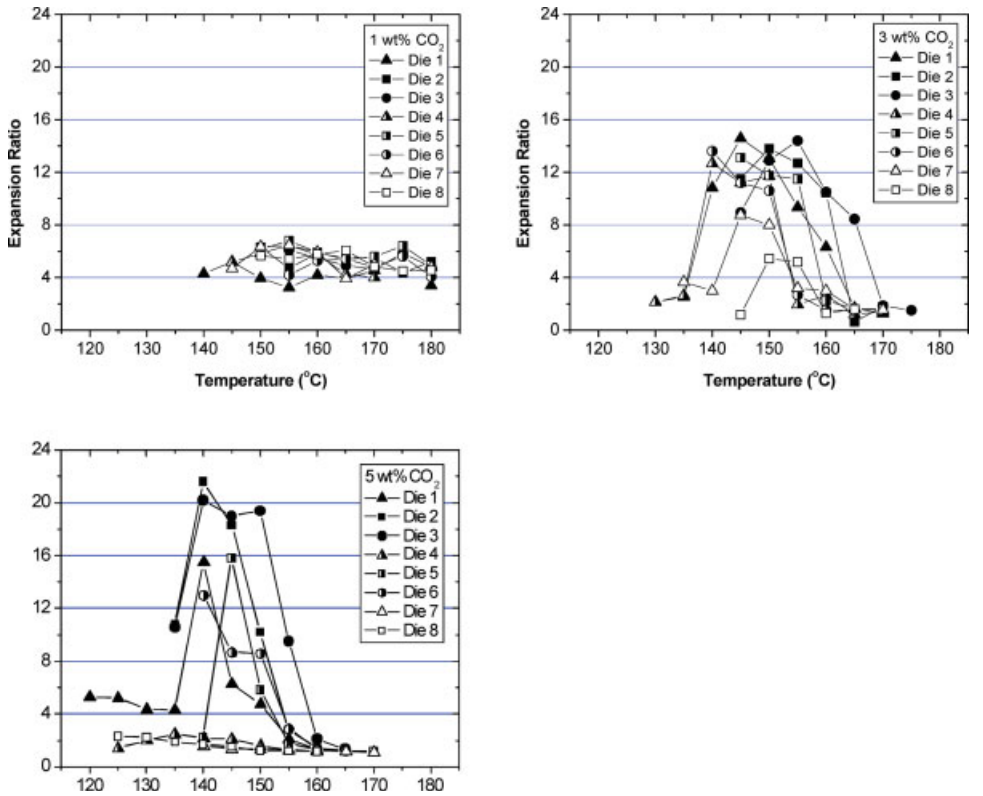

Figure 4 Expansion ratios versus die pressures at: (a) 1 wt % of CO_2, (b) 3 wt % of CO_2, (c) 5 wt % of CO_2. [Color figure can be viewed in the online issue, which is available at www.interscience.wiley.com.]

foaming occurred as the pressure decreased at the die exit. To obtain a constant 12 g/min gas/polymer mixture flow rate, we maintained fixed amounts of the materials and controlled the processing parameters, such as the screw speeds (i.e., 18 RPM for the first screw and 3.5 RPM for the second screw); the gear pump speed (i.e., 13 RPM); the blowing agent content (i.e., 1, 3, or 5 wt %); and the barrel temperatures (i.e., 180, 210, and 205°C for the first screw, and 180°C for the entire length of the second screw). The synchronized melt and die temperatures were lowered step by step, and samples were randomly collected at each set temperature only after the system reached the equilibrium state. The images of the extruded foam profiles were captured with the CCD camera as the temperature was varied.

The solidified foam samples were randomly chosen from each processing condition and characterized using an optical microscope (Wild Heerburgg) and/or a scanning electron microscope (SEM, Hitachi 510). The foam samples were dipped in liquid nitrogen and then fractured to expose the cellular morphology before the foam structure was characterized. Moreover, the volume expansion ratio and the cell population density were measured. The expansion ratio of foam was determined by measuring the weight and volume of the sample. The volume expansion ratio of each sample was calculated as the ratio of the bulk density of pure PP to the bulk density of the foam sample.

RESULTS AND DISCUSSION

The nucleation and volume expansion behaviors of HMS branched PP were investigated for various CO_2 contents (i.e., 1, 3, and 5 wt %) and die geometries (i.e., three die groups) at a fixed talc content (i.e., 0.8 wt %). The obtained results were then plotted for various die geometry and processing parameter combinations. Figures 4 and 5 illustrate the volume expansion ratios and cell densities as a function of the die temperature for all eight dies. The cell structures, observed under SEM, show typical closed-cells with cell walls stretched to thin film at high expansion ratios. The SEM images are similar to previous foaming studies using PP[22,23] and are thus omitted in this paper.

As a case example, the die pressure changes versus the temperature were depicted for 3 wt % CO_2 experiments for all the dies (see Fig. 6). It should be noted that some variations in die pressures were observed among dies that were assigned the same pressure: dies 1, 4, and 7 (i.e., 6.9 MPa), dies 2, 5,

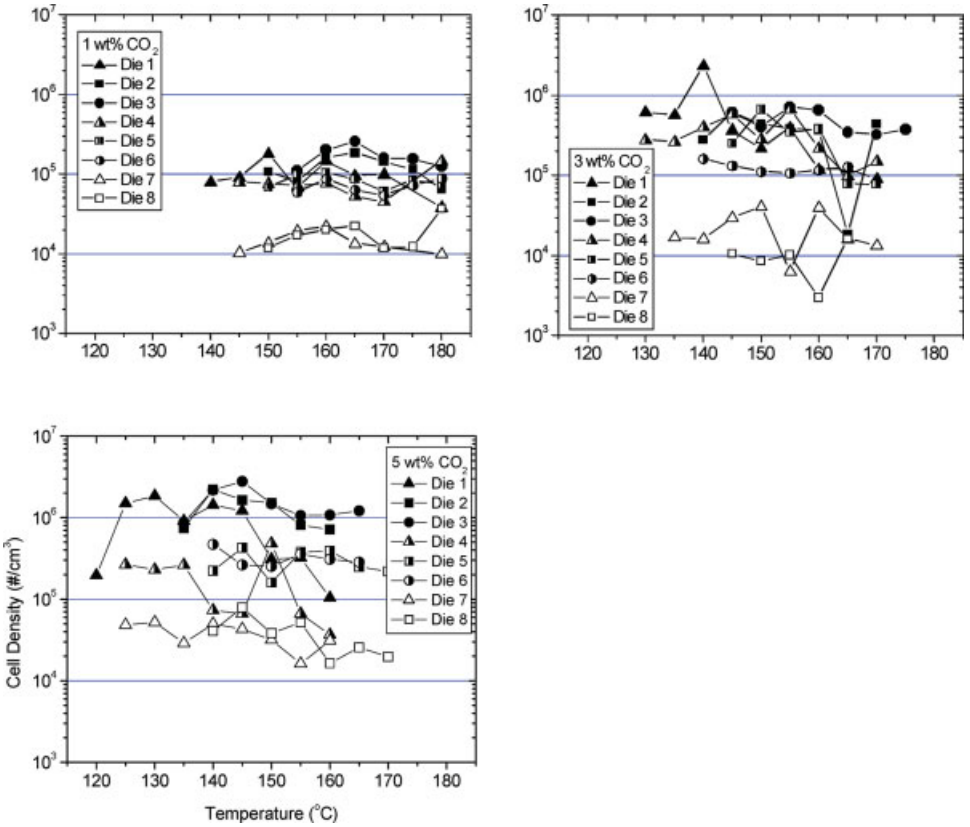

Figure 5 Cell densities versus die pressures at: (a) 1 wt % of CO_2, (b) 3 wt % of CO_2, (c) 5 wt % of CO_2. [Color figure can be viewed in the online issue, which is available at www.interscience.wiley.com.]

and 8 (i.e., 13.8 MPa), and dies 3 and 6 (i.e., 20.7 MPa); It was expected that the dies in each die group (e.g., dies 1, 2, and 3) would have the same pressure drop rate because they each exhibited the same diameter.[52] The CCD images were also collected to investigate the initial expansion behaviors of the PP-CO_2 extrudates; the images are shown in Figure 7.

Effect of die temperature

Volume expansion ratio

Similar to the curve patterns that typically characterize PP and *n*-butane foaming experiments, the expansion ratios of PP foams blown with CO_2 also exhibited mountain-shaped curves [see Fig. 4(b,c)], indicating that the optimum temperature range for reaching maximum expansion was achieved. The expansion ratio was constrained by two major mechanisms: the severe loss of CO_2 through the foam skin at high temperatures, and the crystallization of the polymer matrix at low temperatures, as described earlier. The typical mountain-shaped expansion curves were not observed, however, for the 1 wt % CO_2 experiments [see Fig. 4(a)] due to the lack of gas in the polymer matrix available for foam expansion. Consequently, the maximum expansion ratios were only about sevenfold. It should be noted that the expansion ratios from the lower pressure die experiments (dies 1, 4, and 7) with 5 wt % CO_2 were significantly lower than those characteristic of the higher pressure die experiments. As discussed previously, this was due to a large number of

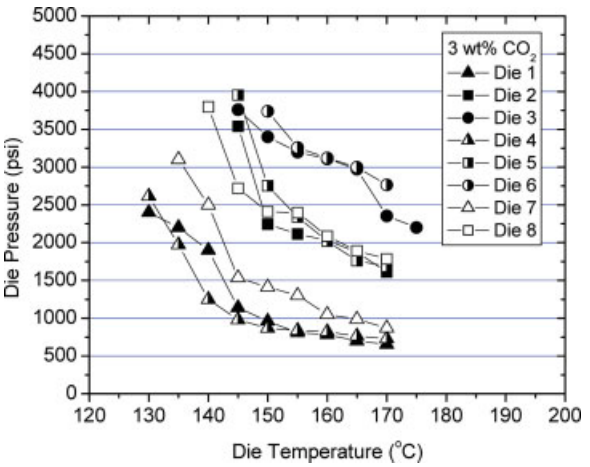

Figure 6 Die pressure profiles at 3 wt % of CO_2. [Color figure can be viewed in the online issue, which is available at www.interscience.wiley.com.]

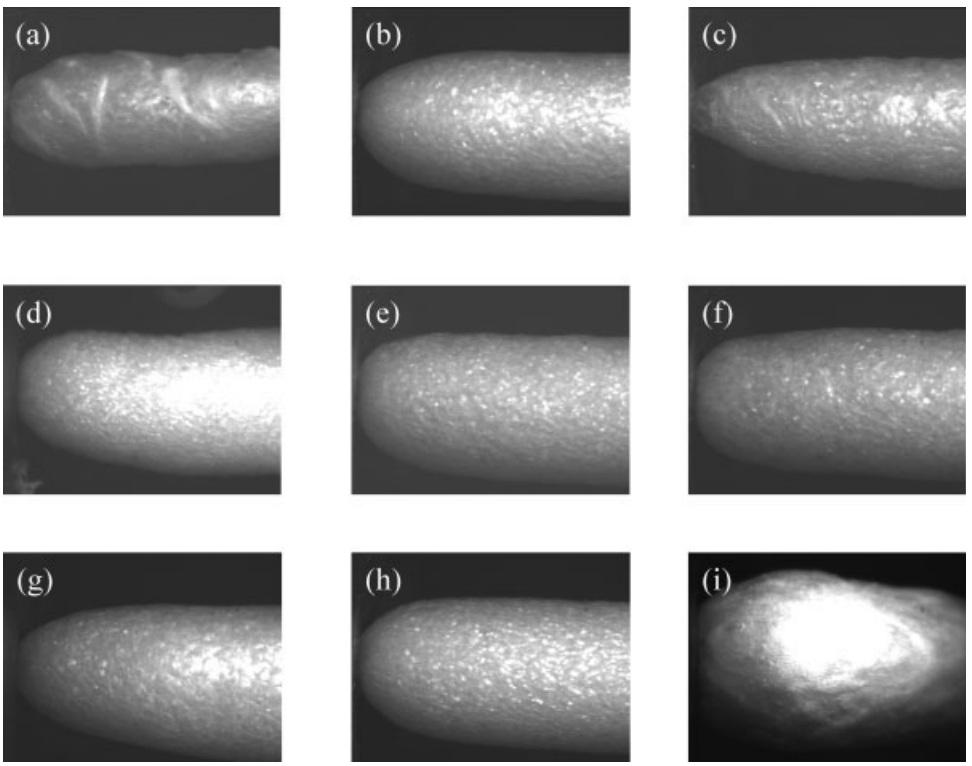

Figure 7 CCD images of extrudates at different CO_2 contents and temperatures: (a) Die 5, 3 wt % CO_2, high T; (b) Die 5, 3 wt % CO_2, medium T; (c) Die 5, 3 wt % CO_2, low T; (d) Die 4, 3 wt % CO_2, 150°C; (e) Die 5, 3 wt % CO_2, 150°C; (f) Die 6, 3 wt % CO_2, 150°C; (g) Die 2, 3 wt % CO_2, 150°C; (h) Die 5, 3 wt % CO_2, 150°C; (i) Die 8, 3 wt % CO_2, 150°C.

undissolved gas pockets in the die land (i.e., $P_{die} < P_{solubility}$).

Cell-population density

The cell population densities were insensitive to the die temperatures as previously observed for other polymer and blowing agent combinations.

Initial expansion behavior

The CCD images of the extruded PP foams taken at various temperatures were analyzed to explore and elucidate their initial expansion behaviors [Figs. 7 (a–c)]. At higher temperatures, the initial expansion rate was significantly high; however, due to high gas diffusivity at this high temperature, the final diameter of the extruded foam was small. As the temperature decreased, the initial expansion rate decreased because of lowered gas diffusivity, whereas the final diameter of the extruded foams increased due to a smaller amount of gas loss. The optimum temperature required to achieve the maximum diameter of the extrudate was determined; it appeared to correspond to the final maximum expansion ratio of the PP foam. When the temperature was decreased further, the diameter of the foam extrudate decreased again due to the crystallization or ''freezing'' of the foam's skin.

Effect of die pressure

Xu and Park[60] have claimed that pressure does not affect the premature cell growth time when the die radius (i.e., the pressure drop rate) is the same. Moreover, they also determined that the degree of premature cell growth is not a function of pressure since the cell population density would be insensitive to the pressure. This means that within the same die groups (i.e., same pressure drop rate), the nucleation and expansion behaviors should be almost similar as long as the die pressures are above the solubility pressure of CO_2 at given conditions. The results featured in Figures 4 and 5 demonstrate that the cell population densities and expansion ratios within the same die group showed little differences, which supports arguments in the background section of this paper. The only exceptions were observed in the low die pressure experiments (Dies 1, 4, and 7) for the same reason discussed above. The CCD images of die Group 2 (Die 4, 5, and 6) with 3 wt % CO_2 experiments showed almost no difference in the initial expansion behaviors among the same pressure drop rate dies [Fig. 7(d–f)].

Effect of die pressure drop rate

Volume expansion ratio

Figure 4(b,c) showed that a high pressure drop rate is favorable to obtain a large expansion ratio for the PP-CO_2 system. As the pressure drop rate decreased from 155 to 7.2 MPa/s (i.e., from die Group 1 to die Group 3), the expansion ratio decreased. The effect of the pressure drop rate became more dramatic as the CO_2 content was increased. Figure 4(c) demonstrates the expansion ratios for three distinctive groups (i.e., each corresponding die group); expansion ratios were observed for all dies, but were exceptionally small in the low-pressure ones (i.e., Dies 1 and 4). The low expansion ratios characteristic of the experiments with Dies 1 and 4 were due to undissolved gas pockets in the die land, as mentioned in the previous section of calculating the amount of premature cell growth.

Two major factors appeared to contribute to the final expansion ratio with respect to the pressure drop rate: (i) the amount of premature cell growth, and (ii) the number of cell layers in the cross section of the extrudate. According to Xu and Park,[60] the amount of premature cell growth in dies that have the highest pressure drop rate are the smallest due to the decreased premature cell growth time. They demonstrated that the maximum expansion ratio obtained from each die decreased as the premature cell growth amount increased. The other factor that may have affected the final expansion ratio was the number of cell layers in the cross section of the extrudate. As the cell population density increased with a higher pressure drop rate, the number of cell layers in the extrudate also increased. Lee and Ramesh[61] have observed an increase in the expansion ratio of extruded LDPE foams with a high cell density due to the localized gas loss in the foam surface area. The same explanation may be applicable to these PP-CO_2 experiments.

Cell-population density

As shown in Figure 5, the cell population density was a very sensitive function of the die pressure drop rate at all CO_2 contents. As the CO_2 content increased from 1 to 5 wt %, the overall cell population densities steadily increased for all eight dies.

Initial expansion behavior

The CCD images of the PP-CO_2 extrudates were collected and analyzed to examine the effect of the die pressure drop rate on the initial expansion behaviors. Figure 7(g–i) illustrate how the initial expansion rate of the extrudate became lower as the pressure drop rate increased. In the experiment with the lowest pressure drop rate (i.e., 7.2 MPa/s for Die 8 [see Fig. 7(i)], an initial hump was observed due to the excessive amount of premature cell growth that occurred in the die. In turn, instant foam expansion transpired immediately after the extrudate exited from the die (represented pictorially by the initial hump); contraction ensued, which led to a low final expansion ratio [see Fig. 4(b)].

SUMMARY AND CONCLUSIONS

In this study, the effects of die geometry on the foaming behavior of PP foams blown with CO_2 in extrusion were investigated. The experiments conducted in this study led to the following conclusions:

1. The curve of the final expansion ratio of PP foam versus temperature showed a typical mountain shape for 3 and 5 wt % CO_2 experiments, indicating that gas loss and melt stiffening were the two governing mechanisms of expansion. The expansion ratios characteristic of 1 wt % CO_2 experiments were only four- to seven-fold over the whole processing temperature range.
2. The effect of die pressure (within the same die group) on nucleation and expansion behavior seemed to be negligible as long as the die pressure remained above the solubility pressure of CO_2.
3. Both the cell population density and the volume expansion ratio increased as the die pressure drop rate increased. The nucleation and expansion behaviors showed little difference within the same die group.
4. The CCD images were utilized to analyze the initial expanding behavior of PP-CO_2 mixture effectively. The trends that emerged from image analysis corresponded strongly with the final foam morphologies.

References

1. Klempner, D.; Frish, K. C. Handbook of Polymeric Foams and Foam Technology; Hanser: New York, 1991.
2. Leaversuch, R. D. Mod Plast 1996, 73, 52.
3. Park, C. B.; Cheung, L. K. Polym Eng Sci 1997, 37, 1.
4. Park, C. P. Polymeric Foams; Hanser: New York, 1991.
5. Baldwin, D. F.; Park, C. B.; Suh, N. P. Polym Eng Sci 1998, 38, 674.
6. Ramesh, N. S. In Foam Extrusion: Principles and Practice; Lee, S. T., Eds.; Technomic: New York, 2000.
7. Naguib, H. E.; Park, C. B.; Reichelt, N. J Appl Polym Sci 2004, 91, 2661.
8. Nojiri, A.; Sawasaki, T.; Koreeda, T. U.S. Patent 4,424,293 (1984).
9. Nojiri, A.; Sawasaki, T.; Konishi, T.; Kudo, T.; Onobori, S. Frukawa Rev 1982, 2, 34.

10. Lee, Y. D.; Wang, L. F. J Appl Polym Sci 1986, 32, 4639.
11. Kitagawa, S.; Nakayama, T.; Isono, M. U.S. Patent 4,766,159 (1987).
12. Bradley, M. B.; Phillips, E. M. SPE ANTEC Tech Pap 1990, 36, 717.
13. Bavaro, V. P. Sch. and Polyolefins Conf., 1995.
14. Van Calster, M. Foamplas 1997, 97, 149.
15. Panzer, U. SPO 98; Houston: Texas, 1998.
16. Ratzsch, M.; Panzer, U.; Hesse, A.; Bucka, H. SPE ANTEC Tech Pap 1999, 45, 2071.
17. Park, J. J.; Katz, L.; Gaylord, N. G. U.S. Patent 5,149,579 (1992).
18. Park, J. J.; Katz, L.; Gaylord, N. G. U.S. Patent 5,116,881 (1991).
19. Feichtinger, K. U.S. Patent 5,929,129 (1999).
20. Thoen, J.; Zhao, J.; Ansema, P.; Hughes, K. Foams 2000, 5, 2000.
21. Park, P. Foamplas 2000, 35, 2000.
22. Naguib, H. E. Ph.D. Thesis, University of Toronto, 2001.
23. Naguib, H. E.; Park, C. B.; Panzer, U.; Reichelt, N. Polym Eng Sci 2002, 42, 1481.
24. Jacob, C.; Dey, S. K. J Cell Plast 1995, 31, 38.
25. Dey, S. K.; Natarajan, P.; Xanthos, M. J. J Vinyl Add Tech 1996, 2, 339.
26. Shimano, T.; Orimo, K.; Yamamoto, S.; Azuma, M. U.S. Patent 3,981,649 (1976).
27. Orimo, K.; Azuma, M.; Shimano, T.; Yamamoto, S. U.S. Patent 3,988,404 (1976).
28. Martini-Vvedensky, J.; Suh, N. P.; Waldman, F. U.S. Patent 4,473,665 (1984).
29. Colton, J. S.; Suh, N. P. U.S. Patent 5,160,674 (1992).
30. Cha, S.; Suh, N. P.; Baldwin, D. F.; Park, C. B. U.S. Patent 5,158,986 (1992).
31. Baldwin, D. F.; Suh, N. P.; Park, C. B.; Cha, S. U.S. Patent 5,334,356 (1994).
32. Park, C. B.; Suh, N. P.; Baldwin, D. F. U.S. Patent 5,866,053 (1999).
33. Park, C. B.; Behravesh, A. H.; Venter, R. D. Polym Eng Sci 1998, 38, 1812.
34. Behravesh, A. H.; Park, C. B.; Venter, R. D. Cell Polym 1998, 17, 309.
35. Park, C. B.; Suh, N. P. Polym Eng Sci 1996, 36, 34.
36. Baldwin, D. F.; Park, C. B.; Suh, N. P. Polym Eng Sci 1996, 36, 1446.
37. Park, C. B.; Baldwin, D. F.; Suh, N. P. Polym Eng Sci 1995, 35, 432.
38. Alteepping, J.; Nebe, J. P. U.S. Patent 4,940,736 (1990).
39. Ahmadi, A. A.; Hornsby, P. R. Plast Rubber Proc Appl 1985, 5, 35.
40. Ahmadi, A. A.; Hornsby, P. R. Plast Rubber Proc Appl 1985, 5, 51.
41. Colton, J. S.; Suh, N. P. U.S. Patent 4,922,082 (1990).
42. Dey, S. K.; Natarajan, P.; Xanthos, M. SPE ANTEC Tech Pap 1996, 42, 1955.
43. Park, C. B.; Cheung, L. K.; Song, S. W. Cell Polym 1998, 17, 221.
44. Fukushima, N.; Kitagawa, Y.; Okumura, T.; Sakakura, K. U.S. Patent 4,522,955 (1982).
45. Holland, R.; Fellers, J. U.S. Patent 3,996,171 (1975).
46. Park, C. P. U.S. Patent 5,527,573 (1994).
47. Park, C. P. U.S. Patent 5,567,742 (1994).
48. Park, C. P. U.S. Patent 5,348,795 (1994).
49. Wilkers, G.; Stimler, J.; Bly, K.; Dunbar, H.; Uhl, E. U.S. Patent 5,817,705 (1996).
50. Naguib, H. E.; Song, S. W.; Park, C. B.; Byon, Y. J. SPE ANTEC Tech Pap 2000, 46, 1867.
51. Naguib, H. E.; Park, C. B.; Lee, P. C.; Xu, D. J Polym Eng 2006, 26, 565.
52. Xu, X.; Park, C. B.; Xu, D.; Pop-Iliev, R. Polym Eng Sci 2003, 43, 1378.
53. Michaeli, W. Extrusion Dies for Plastics and Rubber; Hanser: Munich, 2003.
54. Wang, J.; Park, C. B. SPE ANTEC Tech Pap 2006, 896.
55. Macosko, C. W. Rheology—Principles, Measurements, and Applications; VCH Publishers: New York, 1994.
56. Naguib, H. E.; Park, C. B.; Lee, P. C. J Cell Plast 2003, 39, 499.
57. Xu, X.; Park, C. B. SPE ANTEC Tech Pap 2003, 1823.
58. Li, G.; Wang, J.; Park, C. B.; Simha, R. SAE World Congress, Paper no.2005–01-1671, 2005.
59. Areerat, S.; Funami, E.; Hayata, Y.; Nakagawa, D.; Ohshima, M. Polym Eng Sci 2004, 44, 1915.
60. Xu, X.; Park, C. B. SPE ANTEC Tech Pap 2003, 49, 1058.
61. Lee, S. T.; Ramesh, N. S. SPE ANTEC Tech Pap 1995, 41, 2217.